

# New Varieties of Crystalline Architecture Produced by Small Changes in Molecular Structure in Tape Complexes of Melamines and Barbiturates

Jonathan A. Zerkowski, John P. Mathias, and George M. Whitesides\*

Contribution from the Department of Chemistry, Harvard University, Cambridge, Massachusetts 02138

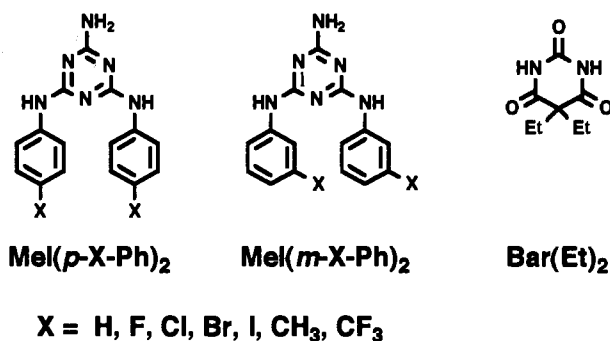
Received October 9, 1992. Revised Manuscript Received March 2, 1994<sup>o</sup>

**Abstract:** This paper describes the crystal structures of a series of seven 1:1 complexes between *N,N'*-bis(*m*-X-phenyl)-melamine and 5,5-diethylbarbituric acid (X = H, F, Cl, Br, I, CH<sub>3</sub>, and CF<sub>3</sub>). This series provides small perturbations on the structures of molecules (*N,N'*-bis(*p*-X-phenyl)melamines) used in a previous study (Zerkowski, J. A.; MacDonald, J. C.; Seto, C. T.; Wierda, D. A.; Whitesides, G. M. *J. Am. Chem. Soc.* In press). Both the *meta* and *para* complexes crystallize as hydrogen-bonded "tapes". With the phenyl substituent in the *meta* position, however, the melamines can adopt a greater number of molecular conformations; this feature leads to a greater variety of orientations of packing. The *meta* series packs in both linear and crinkled tape motifs, and four of the seven complexes are solvates. By contrast, the *para* series, which used the same set of phenyl substituents, always yielded linear tapes and crystals without solvent in the lattice. Inclusion of solvent increases the packing coefficients of members of the *meta* series to values approximately equal to those of the *para* series. The multiplicity of molecular conformations available to the *meta* series is probably largely responsible for the clathration of solvent, which does not rely upon specific non-covalent interactions except in the case of the *m*-iodo complex with acetonitrile. The wider range of crystalline architecture in the *meta* series attests only to the kinetic accessibility of these packing formats; polymorphic phases of greater thermodynamic stability may occur. Polymorphism has not been investigated in the series of *meta*-substituted compounds.

## Introduction

To expand our understanding of the physical–organic chemistry of the solid state, we are continuing to develop a system of co-crystallized derivatives of melamine and of barbituric acid.<sup>1–4</sup> Hydrogen bonding between these components affords crystallographically infinite 1:1 solid-state complexes in the form of "tapes" that pack with their long axes parallel. The constrained packing of tapes allows systematic study of the relationships of crystalline architecture to molecular structure. Formation of the triad of hydrogen bonds that links the components of the tapes withstands variation of the substituents at the periphery of the tapes. We have found that steric properties of the substituents can be controlled to induce selectively the formation of three different crystalline motifs: linear tape (for small substituents),<sup>3</sup> crinkled tape (for medium-sized substituents),<sup>2,4</sup> or cyclic pseudo-C<sub>3</sub> "rosette" structures (for large substituents).<sup>2</sup> These motifs can be thought of as abbreviated segments of the infinite hydrogen-bonded sheet structure of the 1:1 complex between cyanuric acid and melamine (CA·M). We have used the network of hydrogen bonds in the CA·M lattice as the conceptual template for the design of crystallographic motifs<sup>1,3</sup> and solution-phase structures.<sup>5,6</sup>

Our most extensive investigations have focused on a series of *para*-substituted diphenylmelamines complexed with 5,5-diethylbarbituric acid (barbital, Bar(Et)<sub>2</sub>).<sup>3</sup> The principal result from that work was that all the tapes were linear when the *para* substituent was CF<sub>3</sub> or smaller.<sup>7</sup> An important inference from X-ray powder diffraction was that polymorphism occurred for



some of the complexes.<sup>3,8</sup> In the work reported in this paper, we changed the position of substituents on the phenyl rings of the melamine component of the tapes from *para* to *meta*, so that we could explore a structurally closely related series of compounds. We employed the same set of substituents (H, F, Cl, Br, I, CH<sub>3</sub>, and CF<sub>3</sub>) in our investigations of both the *para*- and *meta*-substituted series of complexes so that comparisons between the two series could be as straightforward as possible. The barbiturate component was held constant as Bar(Et)<sub>2</sub> in both series.

While these changes in the pattern of substitution on the diphenylmelamines are geometrically well-defined, they are not necessarily simple. For example, the number of conformers obtainable by rotation around the *N*-phenyl bond in the melamine, which affects both steric and electrostatic features of the molecules, is greater for the *meta* series than for the *para* series.<sup>9</sup> Thus the orientational options for packing the molecules are substantially more complicated for the *meta*- than for the *para*-substituted compounds.

Our overall aim in this work was to survey the crystalline architecture (either new varieties or modified versions of those

\* Abstract published in *Advance ACS Abstracts*, April 1, 1994.

(1) Zerkowski, J. A.; Seto, C. T.; Wierda, D. A.; Whitesides, G. M. *J. Am. Chem. Soc.* 1990, 112, 9025.

(2) Zerkowski, J. A.; Seto, C. T.; Whitesides, G. M. *J. Am. Chem. Soc.* 1992, 114, 5473.

(3) Zerkowski, J. A.; MacDonald, J. C.; Seto, C. T.; Wierda, D. A.; Whitesides, G. M. *J. Am. Chem. Soc.* 1994, 116, 2382.

(4) Zerkowski, J. A.; Whitesides, G. M. *J. Am. Chem. Soc.* Previous paper in this issue.

(5) Seto, C. T.; Whitesides, G. M. *J. Am. Chem. Soc.* 1991, 113, 712.

(6) Seto, C. T.; Whitesides, G. M. *J. Am. Chem. Soc.* 1993, 115, 1321.

(7) In two complexes with larger substituents (X = CO<sub>2</sub>Me and C(CH<sub>3</sub>)<sub>3</sub>), the tapes were sterically forced to adopt either the crinkled or rosette format.<sup>2</sup>

(8) MacDonald, J. C.; Zerkowski, J. A. Unpublished data.

(9) We are describing an effective rotation: when the phenyl groups are adjacent to each other as they are in both linear and crinkled tapes, a *meta* substituent would be expected to hinder rotation around the *N*-phenyl bond relative to a *para* substituent. Different conformations must instead be accessed when the melamine is free in solution (or only partially complexed) and rotation around the *N*-triazine bond has separated the phenyl groups.

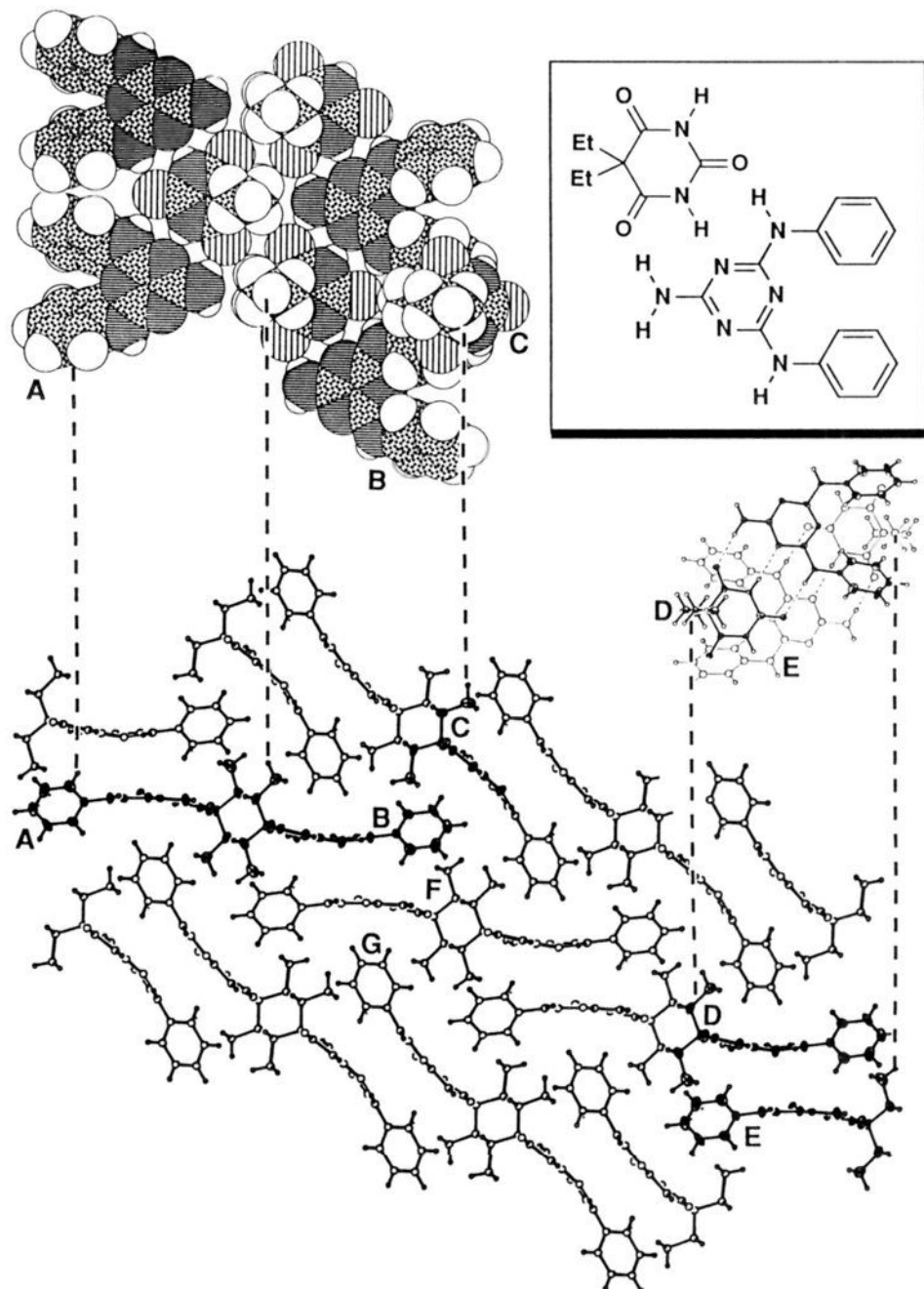


Figure 1. Views of the  $\text{Mel}(\text{Ph})_2\text{-Bar}(\text{Et})_2$  complex.

previously observed) in these *meta*-substituted compounds and to establish the types of structural changes that can accompany a relatively small perturbation on molecular structure.

## Results

To give an overview of the important packing interactions in these co-crystals, we will continue to use the conglomerate pictures (Figures 2–7) that we introduced in previous papers.<sup>3,4</sup> These pictures show several different views of the structure. The complex in which the phenyl substituent is hydrogen (Figure 1, *N,N'*-diphenylmelamine/barbital, or  $\text{Mel}(\text{Ph})_2\text{-Bar}(\text{Et})_2$ ) was discussed fully in an earlier paper.<sup>3</sup> It is included here for comparison to the *meta* series, since it could be considered a member of either the *meta* or *para* series. Table 1 lists crystallographic data and some geometric parameters describing the packing of tapes.

*N,N'*-Bis(*m*-fluorophenyl)melamine/Barbital,  $\text{Mel}(m\text{-F-Ph})_2\text{-Bar}(\text{Et})_2$  (Figure 2). The packing of this complex is similar to

that of the  $\text{Mel}(\text{Ph})_2\text{-Bar}(\text{Et})_2$  complex, although the arrangement of the phenyl groups is significantly different: the melamine molecule does not sit on a mirror plane as it did in  $\text{Mel}(\text{Ph})_2\text{-Bar}(\text{Et})_2$ . One fluorophenyl group is disordered, with 60:40 occupancy of sites related by a  $180^\circ$  rotation of the phenyl ring around the  $\text{FC}_6\text{H}_4\text{-N}$  bond. The corresponding *p*-F complex was also a nonsolvated<sup>10</sup> linear tape, but there were two tapes in its asymmetric unit.

*N,N'*-Bis(*m*-chlorophenyl)melamine/Barbital and *N,N'*-Bis(*m*-bromophenyl)melamine/Barbital,  $\text{Mel}(m\text{-Cl-Ph})_2\text{-Bar}(\text{Et})_2$  and  $\text{Mel}(m\text{-Br-Ph})_2\text{-Bar}(\text{Et})_2$  (Figures 3 and 4). These two structures

(10) We will use the term *solvate* to refer to a specific kind of *clathrate* in which the *host* is the tape complex and the *guest* is the solvent from which it was crystallized. For a proposed scheme of definitions of the varieties of clathrates, see: Weber, E. In *Molecular Inclusion and Molecular Recognition—Clathrates I*; Weber, E., Ed.; Springer-Verlag: Berlin, 1987 (*Top. Curr. Chem.*, Vol. 140).

Table 1. Crystallographic Data for Cocrystals of *N,N'*-Bis(*m*-X-phenyl)melamine and 5,5-Diethylbarbituric Acid, Mel(*m*-X-Ph)<sub>2</sub>Bar(Et)<sub>2</sub><sup>a</sup>

X	solvate	space group	<i>a</i> (Å)	<i>b</i> (Å)	<i>c</i> (Å)	$\alpha$ (deg) <sup>b</sup>	$\beta$ (deg) <sup>b</sup>	$\gamma$ (deg) <sup>b</sup>	<i>R</i> <sup>c</sup>	density (g/cm <sup>3</sup> ) <sup>d</sup>	crystallization solvent	dev from planarity <sup>e</sup> (Å)	tape motif <sup>f</sup>
H		<i>Pnma</i>	12.940	9.982	17.377				0.063	1.369	CH <sub>2</sub> Cl <sub>2</sub>	0.14	L
F		<i>P2<sub>1</sub>/n</i>	9.724	18.715	13.068		93.18		0.085	1.394	CH <sub>3</sub> CN	0.17	L
Cl	1/2 THF	<i>C2/c</i>	27.319	16.656	13.335		119.09		0.044	1.422	THF	0.41	C
Br	1/2 Me <sub>2</sub> CO	<i>C2/c</i>	27.283	16.470	13.340		118.14		0.060	1.632	acetone	0.39	C
I	CH <sub>3</sub> CN	<i>P2<sub>1</sub>/c</i>	13.095	11.575	19.212		96.52		0.033	1.734	CH <sub>3</sub> CN	0.61	L
CH <sub>3</sub>		<i>P1</i>	11.273	12.117	9.730	98.35	110.86	81.45	0.054	1.333	EtOH	0.18	L
CF <sub>3</sub>	CH <sub>3</sub> CN	<i>P2<sub>1</sub>/n</i>	14.268	9.824	22.377		108.18		0.074	1.426	CH <sub>3</sub> CN	0.14	L

<sup>a</sup> The underlined cell dimensions represent the repeat distance in a linear tape. <sup>b</sup> A blank indicates that the angle is constrained to be 90°. <sup>c</sup> This value is the crystallographic reliability index,  $R = \sum |(F_o - F_c)| / \sum F_o$ . <sup>d</sup> Calculated. <sup>e</sup> Deviation from planarity of the hydrogen-bonded backbone (see the text). The average deviation of linear tapes in ref 3 (*para* series) is 0.14 Å. <sup>f</sup> L = linear, C = crinkled.

are isomorphous. The tapes of the complexes are crinkled. There is a CH...O contact (H...O = 2.5 Å,  $\sum_{vdw_{H...O}} = 2.7$  Å) between a proton in the *meta* position of one phenyl ring and a barbituric oxygen in the same tape.<sup>11</sup> Both *meta* complexes are solvates.<sup>12</sup> The crystals of the corresponding *para*-substituted compounds were also isomorphous to each other (for one polymorph of the *p*-X = Br complex), but both of those complexes were nonsolvated linear tapes.

*N,N'*-Bis(*m*-iodophenyl)melamine/Barbital, Mel(*m*-I-Ph)<sub>2</sub>Bar(Et)<sub>2</sub> (Figure 5). The linear tapes of this complex pack as head-to-tail dimers that are further stacked into sheets. The tapes deviate from planarity (Table 1) to a greater extent than any of the linear tapes we observed in the *para* series.<sup>3</sup> Figure 8 shows this deviation in a side-on view of a tape. Solvent (CH<sub>3</sub>CN) is included in the lattice. There is a contact between the nitrogen of acetonitrile and an iodine atom (3.3 Å,  $\sum_{vdw} \sim 3.5$  Å).<sup>13</sup> In the *p*-I complex, which was not a solvate (even when crystallized from acetonitrile), there were extensive I...I contacts under the sum of the van der Waals radii; no such contacts occur in the *m*-I complex.

*N,N'*-Bis(*m*-methylphenyl)melamine/Barbital, Mel(*m*-CH<sub>3</sub>-Ph)<sub>2</sub>Bar(Et)<sub>2</sub> (Figure 6). These linear tapes pack in head-to-tail dimers that then stack into sheets. The *p*-CH<sub>3</sub> analogue was also a nonsolvated linear tape.

*N,N'*-Bis(*m*-(trifluoromethyl)phenyl)melamine/Barbital, Mel(*m*-CF<sub>3</sub>-Ph)<sub>2</sub>Bar(Et)<sub>2</sub> (Figure 7). The tapes of this complex are linear and pack as head-to-tail dimers. Molecules of solvent (CH<sub>3</sub>CN) are included in the lattice in discrete channels between the dimers. This structure is the first example of a channel clathrate that we have observed in crystals of tapes. There are no fluorine-fluorine contacts under the sum of van der Waals radii. There is, however, a region of high fluorine density between tapes B and D in Figure 7. The *p*-CF<sub>3</sub> complex also consisted of linear tapes but was not a solvate.

**Packing Fractions (Table 2).** The *meta* complexes that crystallize as solvates would have lower packing fractions than their *para* congeners if the volume of the solvent molecule were not included in the calculation of  $C_k^*$ .<sup>14</sup> In fact, two of the solvates (*m*-I and CF<sub>3</sub>) would have values lying outside the range accepted as normal for organic molecular crystals.<sup>15</sup> Inclusion of the solvent leads to more efficient packing as measured by minimization of void spaces and maximization of contact of van der Waals surfaces. We comment on the values of  $C_k^*$  in the Discussion section.

(11) We do not know if this contact is attractive or repulsive. For a discussion of CH...O contacts, see: Desiraju, G. R. *Acc. Chem. Res.* 1991, 24, 290.

(12) For Mel(*m*-Cl-Ph)<sub>2</sub>Bar(Et)<sub>2</sub>, the solvent is an ordered molecule of THF; for Mel(*m*-Br-Ph)<sub>2</sub>Bar(Et)<sub>2</sub>, the solvent is a disordered molecule of acetone.

(13) For an investigation of nitrile-iodine interactions, see: Desiraju, G. R.; Harlow, R. L. *J. Am. Chem. Soc.* 1989, 111, 6757.

(14)  $C_k^* = N \cdot V_{mol} / V_{cell}$ , where *N* is the number of molecules in a unit cell,  $V_{mol}$  is the molecular volume, and  $V_{cell}$  is the volume of the unit cell. Kitaigorodsky, A. I. *Organic Chemical Crystallography*; Consultants Bureau: New York, 1961. For a discussion of our modified parameter  $C_k^*$  (calculated using MacroModel), see ref 3.

(15) Values of  $C_k^*$  usually range from roughly 0.65 to 0.77. Desiraju, G. R. *Crystal Engineering: The Design of Organic Solids*; Elsevier: New York, 1989; Chapter 2.

## Discussion

**Crystalline Architecture in the *Meta* Series.** This series of complexes presents examples of several new varieties of the architecture of packing of tapes, as well as modifications of some types that we have observed before. Five of the seven structures (*m*-X = H, F, I, CH<sub>3</sub>, and CF<sub>3</sub>) consist of linear tapes, while the other two (*m*-X = Cl and Br) are crinkled tapes. We have not searched for polymorphism, which was important in the *para* series.<sup>16</sup> Polymorphism may, in fact, also turn out to be crystallographically important in the *meta* series; the greater variety of architecture already observed for complexes of *meta*-substituted diphenylmelamines might suggest that the existence of polymorphs of these complexes is likely.

There are two sets of crystals in which members of the *meta* and *para* series have similar although not isomorphous structures. First, the *m*-CH<sub>3</sub> complex adopts a structure analogous to that of the *p*-Cl and *p*-Br (form I) complexes.<sup>3</sup> All three crystallize in space group *P1* and consist of stacked head-to-tail dimers of tapes. Second, the crinkled tapes of *m*-Cl and *m*-Br pack similarly to the crinkled tape<sup>2</sup> of *p*-CO<sub>2</sub>Me in space group *C2/c*, with solvent included between stacks of tapes.

Another similarity occurs in the packing of the Mel(Ph)<sub>2</sub>Bar(Et)<sub>2</sub> and Mel(*m*-F-Ph)<sub>2</sub>Bar(Et)<sub>2</sub> complexes. In this pair, steric effects seem uppermost in determining packing, since a large change in the dipoles of the substituents does not alter the secondary or tertiary architecture. In addition, the disorder of one of the *m*-fluorophenyl moieties demonstrates the rough steric equivalence of H and F. By contrast, a different result is obtained on going from Mel(Ph)<sub>2</sub>Bar(Et)<sub>2</sub> to Mel(*p*-F-Ph)<sub>2</sub>Bar(Et)<sub>2</sub>. Those two complexes pack with different tertiary architecture.<sup>3</sup>

The adoption of a crinkled tape motif in the *meta* series is not due to the bulk of the substituents. Larger substituents (CH<sub>3</sub> and I) afford linear tapes, while smaller ones (Cl and Br) afford crinkled tapes. It is, however, not clear what factors do determine whether a member of the *meta* series adopts a linear or a crinkled motif. The observation of a particular motif might, in fact, turn out to be a manifestation of polymorphism. In other words, different conditions of crystallization may yield alternative crystalline architectures (such as a crinkled *m*-I or a linear *m*-Br structure).

The Mel(*m*-I-Ph)<sub>2</sub>Bar(Et)<sub>2</sub> complex has a tape backbone that is abnormally deformed, or wavy, for a linear tape (Table 1 and Figure 8). We hypothesize that the deformation of the tapes of this complex reflects association of CH<sub>3</sub>CN and iodine, and not steric properties of the substituent.<sup>13</sup> The tapes incorporating the substituents *m*-CH<sub>3</sub> and *m*-CF<sub>3</sub> (both of which have larger cross sections than I) deviate from planarity to about the same extent as the tapes containing the small substituent *m*-F (see Table 1).

**Importance of Solvent to Packing.** Four of the seven complexes of the *meta* series are solvates: two of the linear tapes (*m*-I and

(16) The principal reason that we have not yet looked for alternative phases of these complexes is that we lack an experimental setup capable of preventing desolvation while investigating the powder diffraction patterns of clathrates. Nonsolvated polymorphs could of course occur, however.

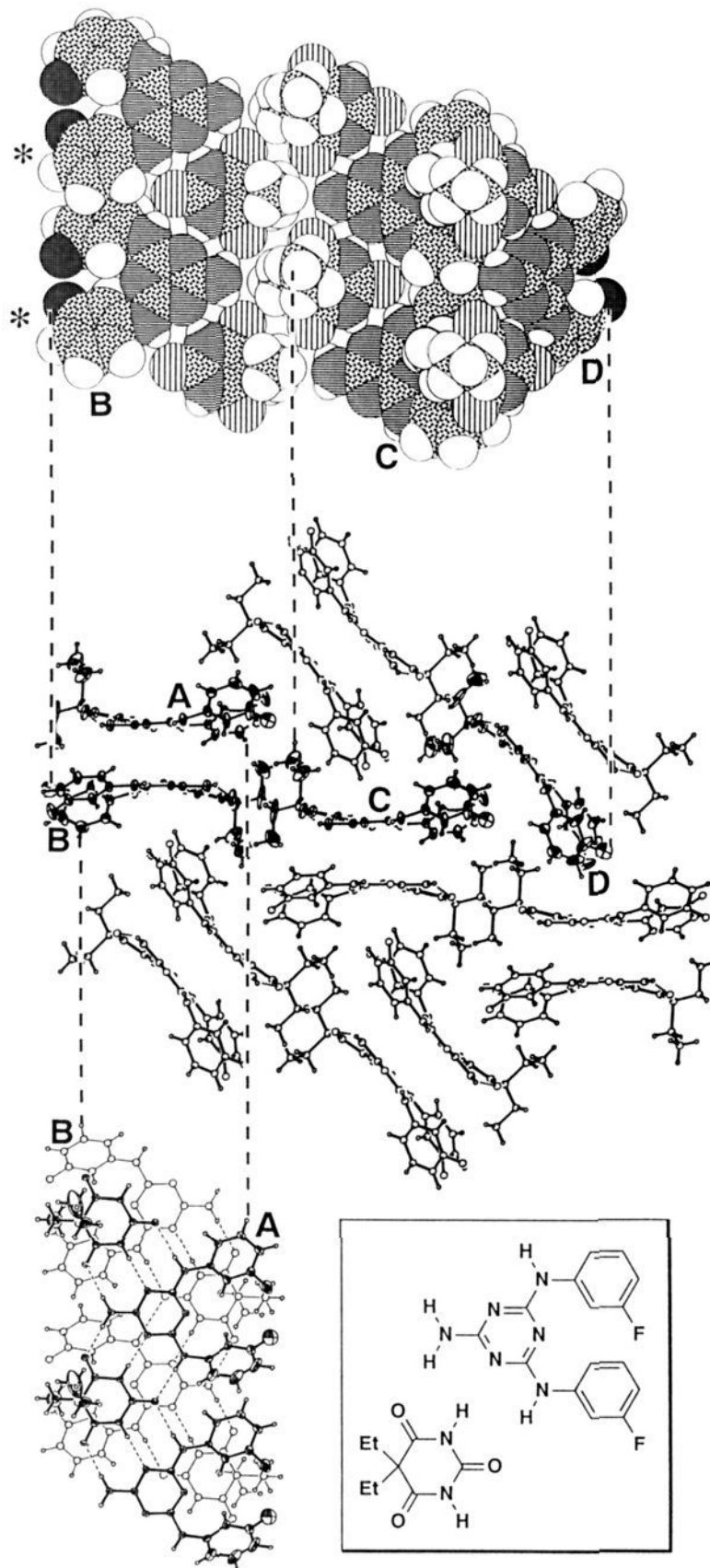


**Figure 2.** Views of the  $\text{Mel}(m\text{-F-Ph})_2\text{Bar}(\text{Et})_2$  complex. One fluorophenyl group (indicated with an asterisk) is disordered; only one position (the one with the more populated fractional site occupancy) is shown for the fluorine in this group.

$m\text{-CF}_3$ ) and both of the crinkled tapes ( $m\text{-Cl}$  and  $m\text{-Br}$ ). By contrast, none of the crystals of linear tapes in the *para*-substituted

series contained solvent. All of these solvated crystals decomposed through the loss of solvent at room temperature in the open

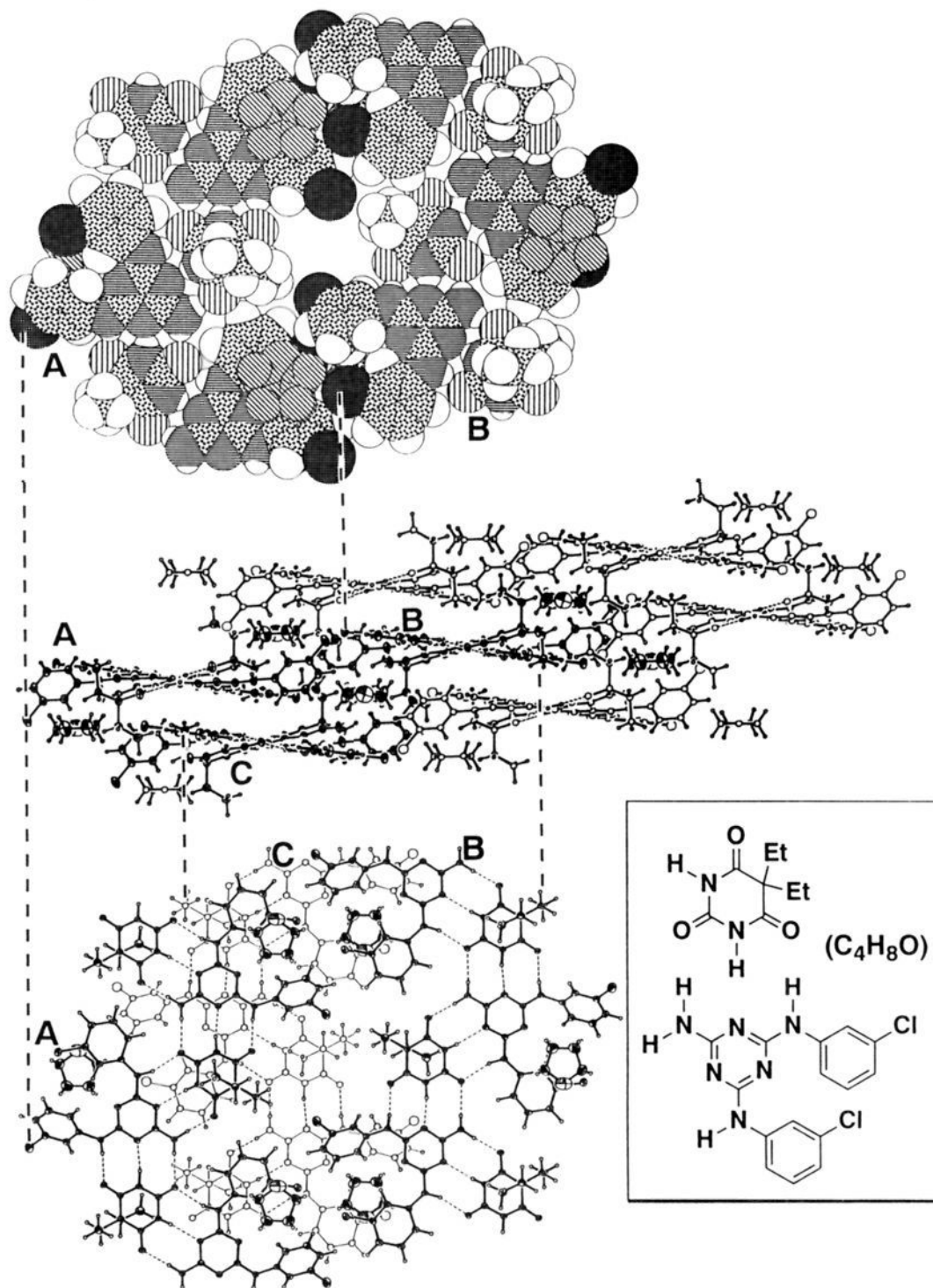


Figure 3. Views of the Mel(*m*-Cl-Ph)<sub>2</sub>-Bar(Et)<sub>2</sub>·0.5THF complex.

atmosphere, as evidenced by their transformation from clear to opaque and by the development of fractures. The *m*-CF<sub>3</sub> complex desolvated in a matter of hours, *m*-Cl and Br in about a day, and *m*-I over the course of several days. For clathrates, the guest is an integral part of the lattice. It might be most accurate, therefore, to describe these crystals as three-component systems composed of melamine, barbituric acid, and solvent molecules. Solvent seems to play an important role in determining the packing of these tapes (probably more important than that it plays in crystallizations of nonsolvates).

The precise influence of solvent in determining the packing of the *meta* structures remains obscure. The *m*-I solvate is the only

structure that has a specific non-covalent interaction (CN---I) between solvent and host. The crinkled solvates, *m*-Cl and *m*-Br, have contacts between hydrogen atoms of the solvent and halogen atoms (in the range of 2.9 to 3.0 Å) that are just at the limit of van der Waals contact (approximately 2.95 to 3.05 Å), but these interactions are probably weak. Since voids in these two isomorphous crystals are filled by different solvents (THF and acetone), we infer that shape specificity of host for guest is minimal. In the *m*-CF<sub>3</sub> case, there is no host-guest contact, but there is a H---N contact (2.5 Å,  $\Sigma_{vdw} \sim 2.7$  Å) between adjacent solvent molecules, creating a crystallographically infinite chain that may be held together by weak hydrogen bonds. We have

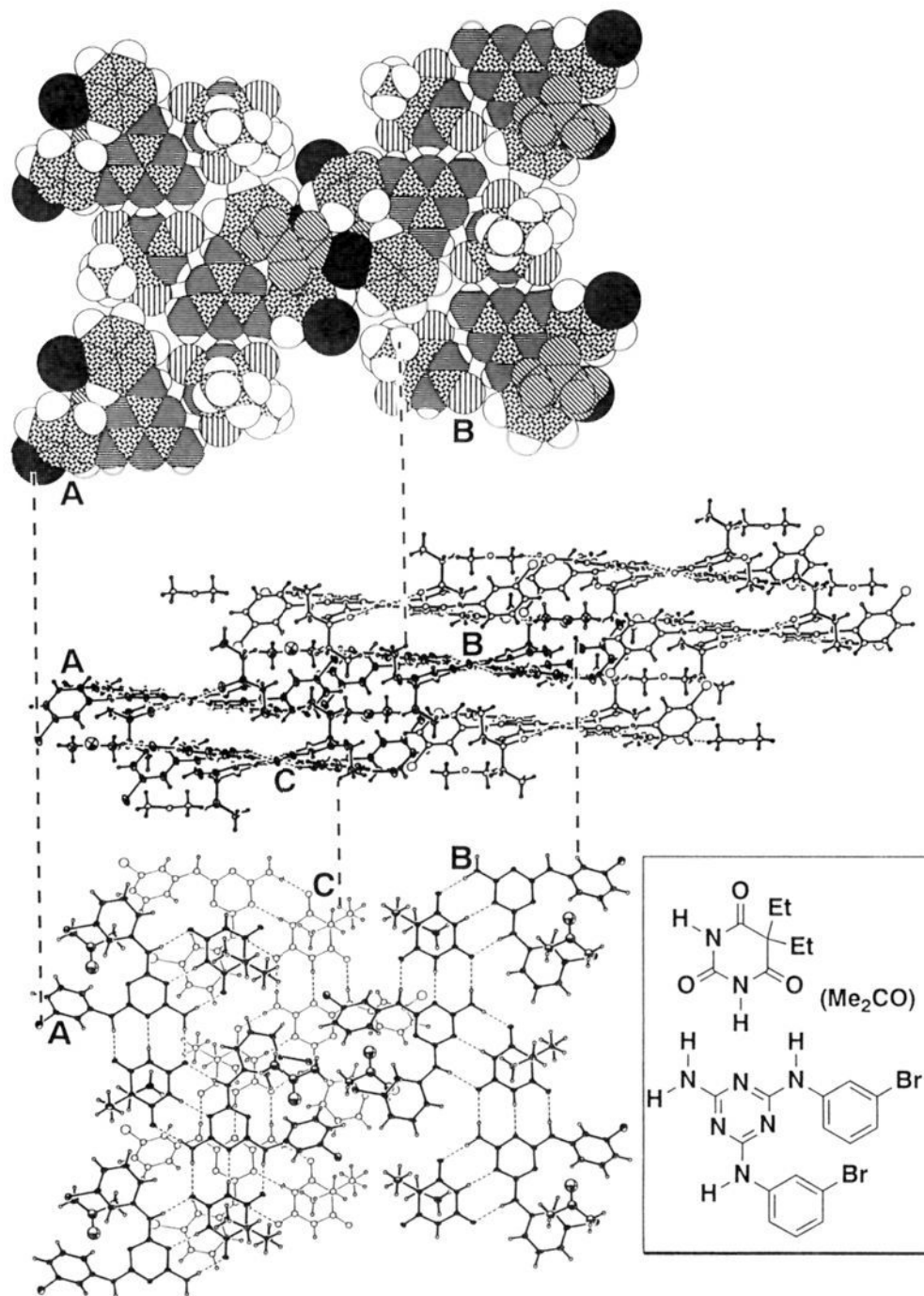


Figure 4. Views of the  $\text{Mel}(m\text{-Br-Ph})_2\text{Bar}(\text{Et})_2 \cdot 0.5(\text{Me}_2\text{CO})$  complex. Only one orientation of the disordered acetone molecule is shown.

not yet investigated the contribution of solvent by attempting to crystallize these complexes (especially the solvates) from different solvents.

For the *para* series, we searched for polymorphism by performing X-ray powder diffraction (XPD) on crystals of the complexes grown from different solvents. While polymorphism occurred unambiguously for *p*-Br and *p*-CF<sub>3</sub>, there was never a special relationship between solvent and crystalline phase in the sense that polymorph X was only obtainable from solvent X or that solvent Y yielded only polymorph Y.<sup>17</sup> In particular, there appeared to be no specific interaction between CH<sub>3</sub>CN and the *p*-I complex when it was grown from that solvent.<sup>8</sup> The crystals were not solvates, and they had the same structure (according to XPD) as crystals grown from other solvents. Similarly, neither

*p*-Cl grown from THF nor *p*-Br grown from acetone were solvates, unlike their *meta* analogues. Observation of solvent-dependent polymorphism in the *meta* series would therefore constitute a marked difference from the *para* series.

Table 2 compares values of the packing coefficient,  $C_k^*$ , for the *para* and *meta* series. In most cases, the value for the *meta* complexes is the same or only slightly larger than that for the *para* complexes. The exception is the pair of CH<sub>3</sub>-substituted complexes. The *meta*-CH<sub>3</sub> complex has a higher value of  $C_k^*$  and is also more dense. The space-filling of the *meta* series is,

(17) Polymorphism of the *p*-Br complex (and perhaps of the *para*-CF<sub>3</sub> complex) appeared to be more sensitive to the rate of crystal growth by solvent evaporation, or to factors influencing nucleation (such as vibrations or dust particles) over which we exercised little or no control, than to the solvent from which the crystals formed (MacDonald, J. C.; Weissbecker, C.; Zerkowski, J. A. Unpublished data).

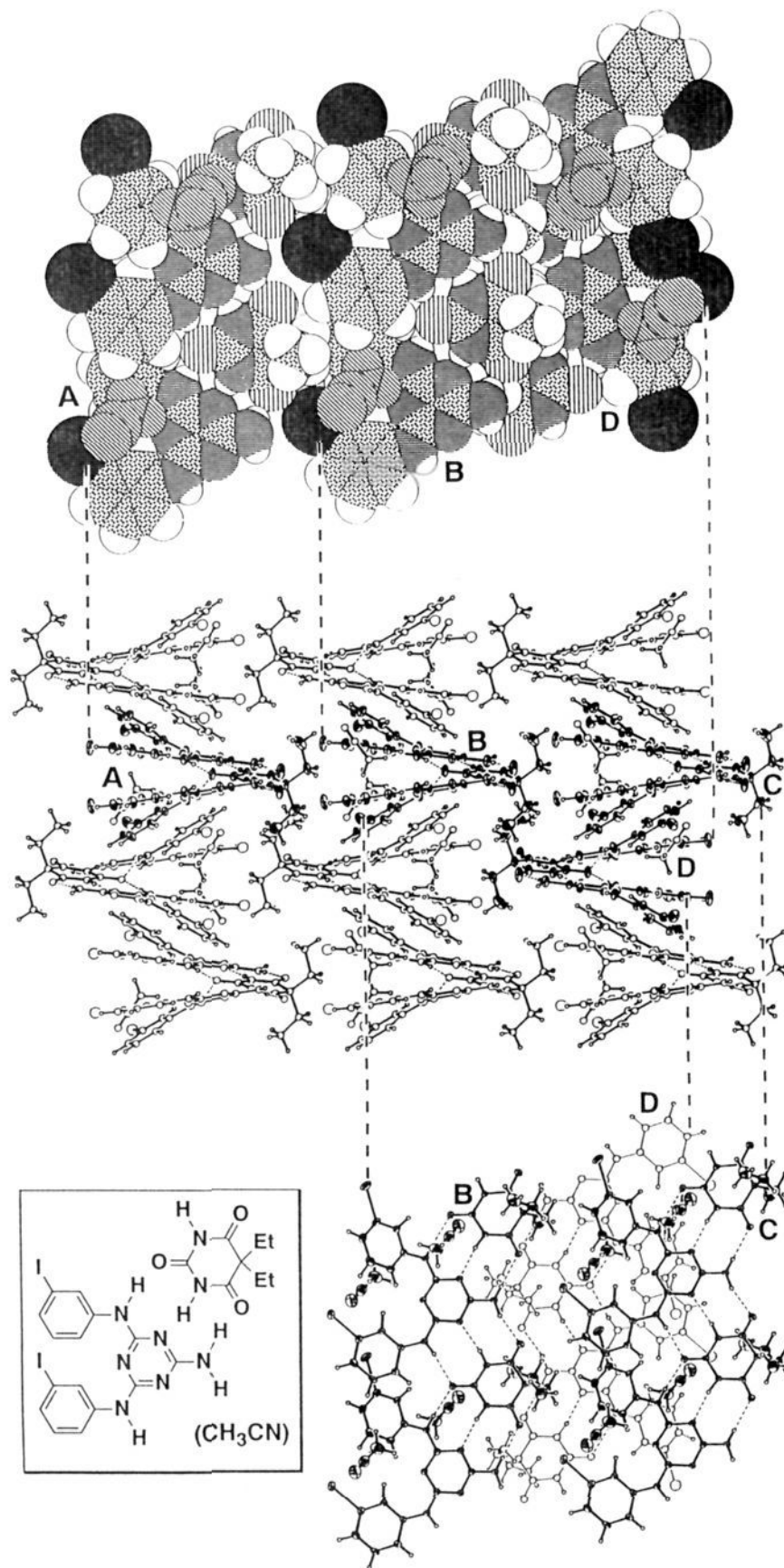


Figure 5. Views of the Mel(*m*-I-Ph)<sub>2</sub>-Bar(Et)<sub>2</sub>-CH<sub>3</sub>CN complex.

therefore, not necessarily less efficient than that of the *para* series. Table 2 also includes a listing of *hypothetical*  $C_k^*$  values for the *meta* solvates with solvent removed. It is interesting that

inclusion of solvent increases the efficiency of space-filling for the *meta* series only to values roughly equal to those of the *para* series.

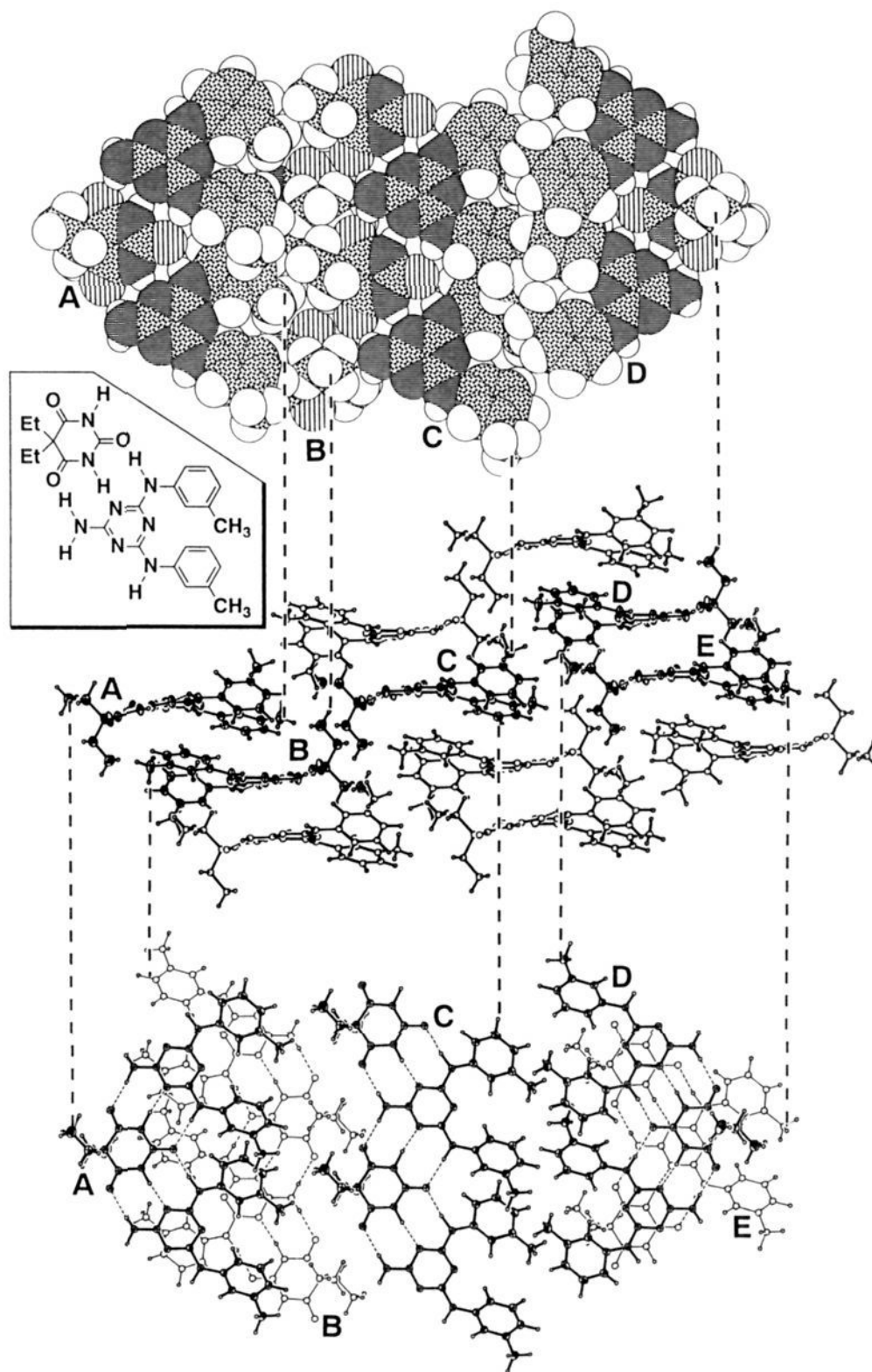


Figure 6. Views of the Mel(*m*-CH<sub>3</sub>-Ph)<sub>2</sub>-Bar(Et)<sub>2</sub> complex.

### Conclusions

A comparison of the series of *meta*-substituted diphenylmelamines complexed with barbital presented in this paper to the *para*-substituted series<sup>3</sup> shows that small changes in molecular structure can be accompanied by significant changes in crystalline architecture. For example, switching a chlorine substituent from a *para* to a *meta* position on a phenyl ring results in a change in the tape motif from linear to crinkled. We emphasize, however,

that we do not know whether this change reflects thermodynamic or kinetic factors (or both). Without extensive studies of polymorphism, the observation of these two particular chlorine-containing structures shows only that both are *accessible*, not that they are thermodynamically preferred relative to other structures.

The *meta* series provides new examples of the varieties of crystalline architecture that tapes, particularly linear ones, can



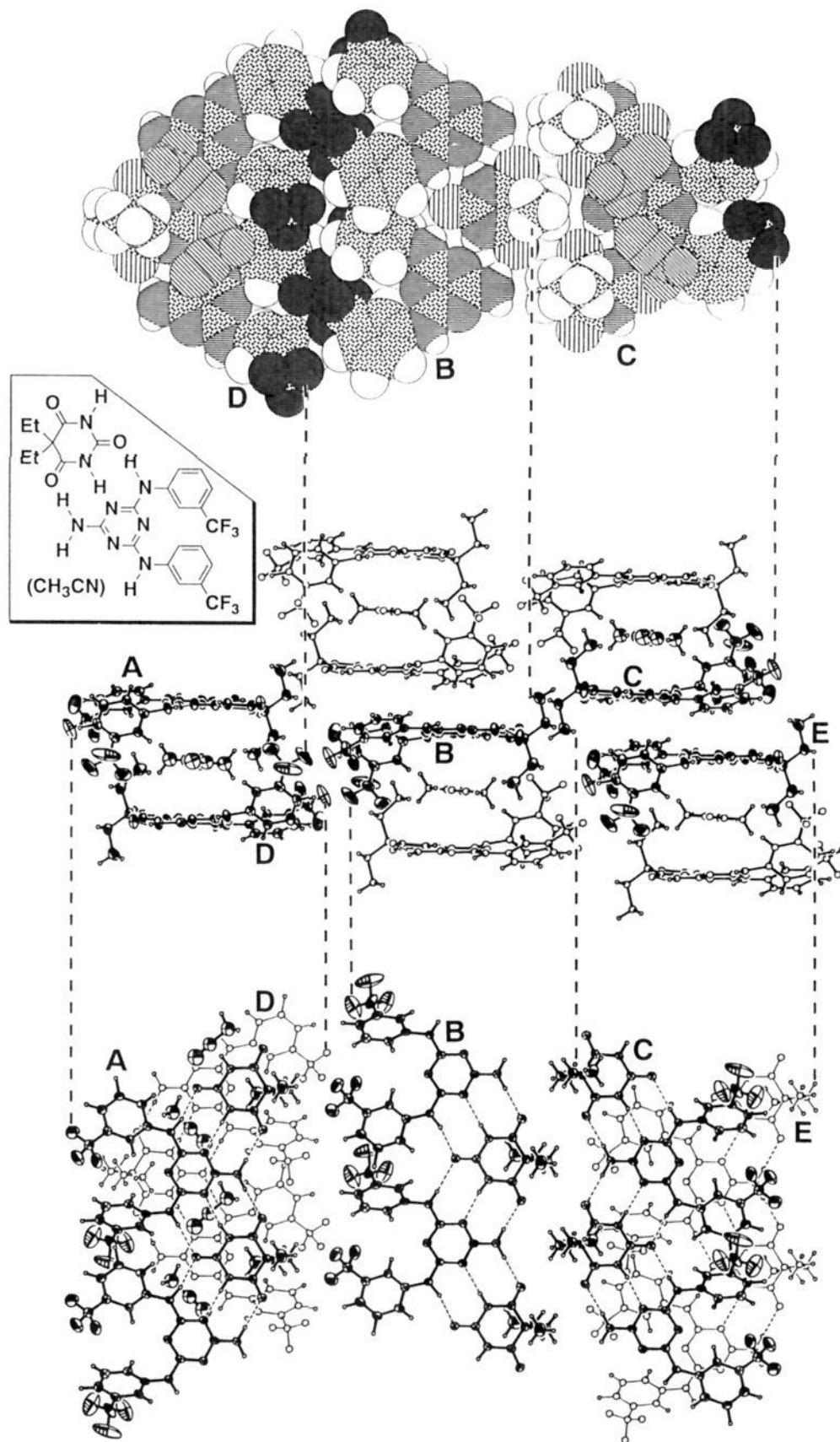


**Figure 7.** Views of the Mel(*m*-CF<sub>3</sub>-Ph)<sub>2</sub>-Bar(Et)<sub>2</sub>-CH<sub>3</sub>CN complex. Tapes can accommodate solvent in the lattice in several ways. First, crinkled tapes (such as *m*-Cl and Br) can pack to give pockets between stacks of tapes that solvent can fill. Second, linear tapes (*m*-I) can deform from planarity (become "wavy")

to allow a solvent molecule to engage in a close, specific contact with a tape substituent. Third, linear tapes (*m*-CF<sub>3</sub>) can pack with channels of solvent between them. In each of these cases, inclusion of solvent increased the efficiency of space-filling of the

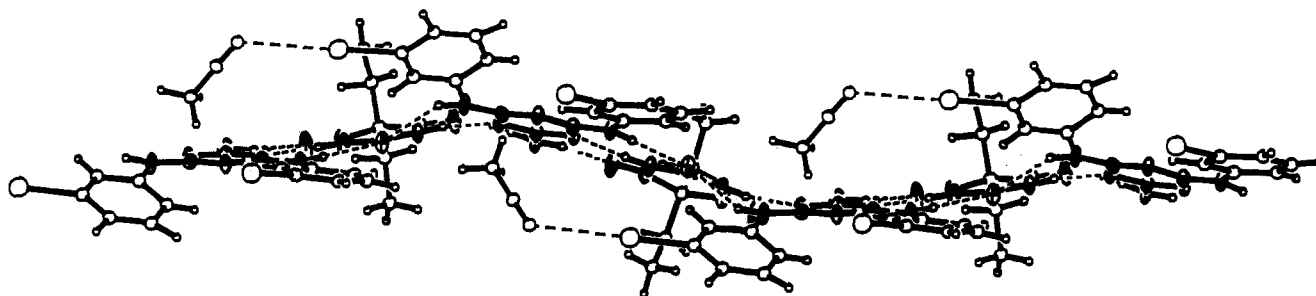


Figure 8. Side view of a tape of the  $\text{Mel}(m\text{-I-Ph})_2\text{-Bar}(\text{Et})_2\text{-CH}_3\text{CN}$  complex showing the deviation from planarity of the tape backbone. The contact between acetonitrile and iodine is indicated by a dashed line. The atoms of the tape backbone are shown as thermal ellipsoids.

Table 2. Comparison of Packing Coefficients for the *Meta* and *Para* Series<sup>a</sup>

X	$C_k^*$ for <i>p</i> -X <sup>b</sup>	$C_k^*$ for <i>m</i> -X	
		with solvent if present	hypothetical, without solvent <sup>c</sup>
H	0.72	0.72	
F	0.69	0.69	
Cl ( $1/2$ THF)	0.70	0.70	0.65
Br ( $1/2$ Me <sub>2</sub> CO)	0.71 (form I) 0.69 (form II)	0.71	0.67
I (CH <sub>3</sub> CN)	0.69	0.70	0.63
CH <sub>3</sub>	0.68	0.71	
CF <sub>3</sub> (CH <sub>3</sub> CN)	0.66	0.67	0.61

<sup>a</sup> These packing coefficients are based on molecular volumes calculated with MacroModel. See ref 3 for a discussion of the relationship between  $C_k^*$  and the packing coefficient calculated in a traditional way,  $C_k$ .<sup>14</sup> <sup>b</sup> Taken from ref 3. <sup>c</sup> This value is a hypothetical one that excludes the contribution to volume from the included solvent molecule.

*meta* series to values approximately equivalent to those of the *para* series. Only the *m*-I complex relies clearly upon a specific host-solvent contact to favor clathration.

We suspect that nonspecific clathration of solvent may arise principally as an effect of polymorphism. For example, since the linear motif can accommodate *meta* substituents with large diameters (I, CH<sub>3</sub>, CF<sub>3</sub>), there should be no steric barrier to the *m*-Br or *m*-Cl complexes adopting a linear motif. Thus there could well be other (yet unobserved) polymorphs, such as linear *m*-Br and *m*-Cl tapes, that pack to fill space more completely but that are not solvates. These phases might occur if crystals were grown from a solvent that for some reason (probably steric) could not be included in a lattice of tapes. Kinetic effects leading to packing arrangements that are local minima in free energy should become more important as conformational multiplicity increases.<sup>18</sup> Computational modeling and energy calculations will be required to make comparisons between alternative packing orientations.

The *meta* series of complexes has important structural similarities to the corresponding *para* series, and to other related 1:1 co-crystalline complexes that we have investigated. In particular, members of this series preserve the triad of hydrogen bonds between melamine and barbituric acid components as the dominant structure-determining element in the solid state and crystallize in both the linear and crinkled tape motifs observed previously. Our initial investigations into this series suggest to us, however, that crystals based on *meta*-substituted diphenylmelamines are less suitable than other series we have examined (specifically, crystals based on *para*-substituted diphenylmelamines<sup>3</sup> and on *N,N'*-di(*tert*-butyl)melamine<sup>4</sup>) as the basis for a systematic physical-organic study. This unsuitability arises because of the greater number of varieties of packing adopted by the *meta* series than by the *para* series. We hypothesize that this range of architectures may be attributable to the variability of molecular conformation of *meta*-substituted diphenylmelamines,<sup>18</sup>

(18) Desiraju, G. R. *Crystal Engineering: The Design of Organic Solids*; Elsevier: New York, 1989; Chapter 10.

while the limited architecture of the *para* series and the *N,N'*-di(*tert*-butyl)melamine series is a result of the reduced conformational multiplicity of those molecules.

## Experimental Section

**General.** All anilines were obtained from Aldrich Chemicals. General procedures were performed as previously published.<sup>3</sup>

**General Procedure for Synthesis of 2-Amino-4,6-bis(arylamino)-1,3,5-triazines (*N,N'*-Diphenylmelamines).**<sup>19</sup> A 0.1 M solution of cyanuric chloride was prepared in freshly distilled THF and cooled in an ice-water bath. A THF solution of 1 equiv of the aniline (0.1 M) and 1 equiv of diisopropylethylamine as base was added from a dropping funnel over the course of 15–30 min with magnetic stirring of the reaction mixture. When the addition was complete, the mixture was allowed to warm to room temperature, and stirring was continued for another hour. The mixture was heated to 40–50 °C in an oil bath, and another equivalent each of aniline and base (in THF) was added. Heating was continued for several hours. At this stage, the intermediate 2-chloro-4,6-diamino-1,3,5-triazine was pure enough, as determined by TLC, that it could be isolated by filtering the reaction mixture through a short plug of silica gel. The silica gel was washed with solvent (ethyl acetate or THF) and the combined organic solutions were concentrated to dryness by rotary evaporation at aspirator pressure. An alternative procedure was to remove the solvent from the reaction mixture by rotary evaporation, dissolve the residue in ethyl acetate and wash it several times with H<sub>2</sub>O, and then remove the ethyl acetate by rotary evaporation. The crude product was used directly in the next step.

The 2-chloro-4,6-diamino-1,3,5-triazine (dissolved in approximately 5–8 mL of 1,4-dioxane or THF) and a magnetic stirrer were placed in a 15-mL pressure bottle. Approximately 3–5 mL of 30% NH<sub>4</sub>OH was added, and the bottle was capped and heated (CAUTION: behind a safety shield) to 100–105 °C in an oil bath. Heating was continued for 5–8 h, after which the vial was cooled and opened to measure the progress of the reaction by TLC. If an unacceptable amount of starting material remained, an additional portion of 30% NH<sub>4</sub>OH (2–3 mL) was added, and the vial was recapped and reheated. When reaction was judged to be complete by TLC, the solution was poured into 150–200 mL of H<sub>2</sub>O, and the precipitated product was collected by vacuum filtration. After drying under vacuum at 0.1 Torr, the crude melamine was purified by flash chromatography on silica gel.

The melting points of the melamines were the following:  $\text{Mel}(m\text{-F-Ph})_2$ , 178–80 °C;  $\text{Mel}(m\text{-Cl-Ph})_2$ , 181–84 °C;  $\text{Mel}(m\text{-Br-Ph})_2$ , 192–95 °C;  $\text{Mel}(m\text{-I-Ph})_2$ , 188–91 °C;  $\text{Mel}(m\text{-CH}_3\text{-Ph})_2$ , 138–40 °C (lit.<sup>20</sup> mp 139–40 °C);  $\text{Mel}(m\text{-CF}_3\text{-Ph})_2$ , 70–75 °C. For spectroscopic details and elemental analyses on new compounds see the supplementary material.

**Preparation of Complexes.** Equimolar amounts of the melamine and barbital were dissolved together (in one flask) in THF. The solvent was removed by rotary evaporation at aspirator pressure, and the composition of the complex was checked by <sup>1</sup>H NMR spectroscopy. If integration of peaks indicated that one component was present in excess, the other component was added to bring their ratio to 1:1. The melting points of the complexes were the following:  $\text{Mel}(m\text{-F-Ph})_2\text{-Bar}(\text{Et})_2$ , 230–32 °C;

(19) This procedure is a modification of that found in: Kaiser, D. W.; Thurston, D. J.; Dudley, J. R.; Schaefer, F. C.; Hechenbleikner, I.; Holm-Hansen, D. *J. Am. Chem. Soc.* **1951**, *73*, 2984.

(20) Honda, I. *Yuki Gosei Kagaku Kyokai Shi* **1962**, *20*, 460; *Chem. Abstr.* **1963**, *58*, 4568c.

Mel(*m*-Cl-Ph)<sub>2</sub>Bar(Et)<sub>2</sub>,<sup>21</sup> 210–12 °C dec; Mel(*m*-Br-Ph)<sub>2</sub>Bar(Et)<sub>2</sub>,<sup>21</sup> 191–94 °C; Mel(*m*-I-Ph)<sub>2</sub>Bar(Et)<sub>2</sub>,<sup>21</sup> 197–202 °C; Mel(*m*-CH<sub>3</sub>-Ph)<sub>2</sub>Bar(Et)<sub>2</sub>, 198–200 °C; Mel(*m*-CF<sub>3</sub>-Ph)<sub>2</sub>Bar(Et)<sub>2</sub>,<sup>21</sup> 178–81 °C. The melting point of barbital is 190–92 °C.

**Crystallization of Complexes:** Mel(*m*-CH<sub>3</sub>-Ph)<sub>2</sub>Bar(Et)<sub>2</sub>. Crystals were grown by room-temperature evaporation of a solution of the complex in EtOH. A slow rate of evaporation (approximately 2 weeks for complete evaporation of solvent from a 1-mL sample of solution) was achieved by enclosing a loosely capped 1-dram screw-top vial containing the solution inside a 10-mL vial that was also loosely capped.

Mel(*m*-F-Ph)<sub>2</sub>Bar(Et)<sub>2</sub>, Mel(*m*-I-Ph)<sub>2</sub>Bar(Et)<sub>2</sub>, and Mel(*m*-CF<sub>3</sub>-Ph)<sub>2</sub>Bar(Et)<sub>2</sub>. Crystals were grown by allowing a solution of the complex in boiling CH<sub>3</sub>CN to cool over the course of at least 24 h to room temperature. A slow rate of cooling was achieved by enclosing a round-bottomed flask containing the solution in a corked Dewar flask. After it was observed that crystals of the *m*-I and *m*-CF<sub>3</sub> complexes were solvates, these crystals were stored in contact with mother liquor.

Mel(*m*-Cl-Ph)<sub>2</sub>Bar(Et)<sub>2</sub> and Mel(*m*-Br-Ph)<sub>2</sub>Bar(Et)<sub>2</sub>. Crystals were grown by room-temperature evaporation of solutions of the complexes in THF and acetone, respectively, in loosely capped 25-mL round-bottomed flasks. Once suitable single crystals had formed, as determined by observation under a microscope, the flasks were tightly stoppered to retain a small amount of solvent and prevent decomposition of the solvated crystals.

(21) The crystalline samples used for melting point analyses of these complexes had been grown from the solvent that afforded the solvated crystals studied by single-crystal diffraction, but they had desolvated prior to the melting point analysis. If solvated samples had been used, they probably would have desolvated (even in a sealed capillary) during the melting point analysis.

**X-ray Crystallography.** For details of X-ray data collection and structure solution and refinement, see the supplementary material. Data were collected on complexes of Mel(*m*-Cl-Ph)<sub>2</sub>Bar(Et)<sub>2</sub> and Mel(*m*-Br-Ph)<sub>2</sub>Bar(Et)<sub>2</sub> at Harvard on a Siemens P3 diffractometer. Data on the other complexes were collected by Molecular Structure Corp., The Woodlands, TX, on a Rigaku AFC5R diffractometer equipped with a rotating anode generator. All structures were solved and refined at Harvard using the Siemens SHELXTL-PLUS package of programs.

**Acknowledgment.** We acknowledge the support of the National Science Foundation through Grants CHE-91-22331 to G.M.W. and CHE-80-00670 to the Department of Chemistry for the purchase of the Siemens X-ray diffractometer. J.P.M. acknowledges support from a SERC/NATO postdoctoral fellowship, 1991–93. We thank Dr. Derk Wierda for helpful discussions.

**Supplementary Material Available:** Experimental details for melamines, crystallographic details including tables of atomic positional parameters and bond lengths and angles (95 pages); tables of observed and calculated structure factors (85 pages). This material is contained in many libraries on microfiche, immediately follows this article in the microfilm version of the journal, and can be ordered from the ACS; see any current masthead page for ordering information.